

Charge transport in underdoped bilayer cuprates

Feng Yuan

*Department of Physics, Beijing Normal University, Beijing 100875, China
The Abdus Salam International Centre for Theoretical Physics, 34014 Trieste, Italy*

Jihong Qin and Shiping Feng

*Department of Physics and Key Laboratory of Beam Technology and Material Modification, Beijing Normal University, Beijing 100875, China
Interdisciplinary Center of Theoretical Studies, Chinese Academy of Sciences, Beijing 100080, China
National Laboratory of Superconductivity, Chinese Academy of Sciences, Beijing 100080, China*

Wei Yeu Chen

*Department of Physics, Tamkang University, Tamsui 25137, Taiwan
(Received 13 November 2002)*

Within the t - J model, we study the charge transport in underdoped bilayer cuprates by considering the bilayer interaction. Although the bilayer interaction leads to the band splitting in the electronic structure, the qualitative behavior of the charge transport is the same as in the case of single layer cuprates. The conductivity spectrum shows a low-energy peak and the unusual midinfrared band. This midinfrared band is suppressed severely with increasing temperatures, while the resistivity in the heavily underdoped regime is characterized by a crossover from the high temperature metallic-like to the low temperature insulating-like behaviors, which are consistent with the experiments.

74.20.Mn, 74.25.Fy, 74.72.-h

It has become clear in the past ten years that cuprate superconductors are among the most complex systems studied in condensed matter physics^{1,2}. The complications arise mainly from (1) strong anisotropy in the properties parallel and perpendicular to the CuO_2 planes which are the key structural element in the whole cuprate superconductors, and (2) extreme sensitivity of the properties to the compositions (stoichiometry) which control the carrier density in the CuO_2 plane, and therefore the regimes have been classified into the underdoped, optimally doped, and overdoped, respectively^{1,2}. In the underdoped and optimally doped regimes, the experimental results³ show that the ratio of the c -axis and in-plane resistivities $R = \rho_c(T)/\rho_{ab}(T)$ ranges from $R \sim 100$ to $R > 10^5$, which reflects that the charged carriers are tightly confined to the CuO_2 planes. This large magnitude of the resistivity anisotropy also leads to the general notion that the physics of doped cuprates is almost entirely two-dimensional, and can be well described by a single CuO_2 plane⁴. However, this picture seems to be incompatible with the fact that the superconducting transition temperature T_c is closely related to the number of CuO_2 planes per unit cell, with single layer compounds of a family generically having lower T_c than bilayer or trilayer compounds². Additionally, there are some subtle differences of the magnetic behaviors between doped single layer and bilayer cuprates. By virtue of systematic studies using NMR and μSR techniques, particularly the inelastic neutron scattering, only incommensurate neutron scattering peaks for the single layer lanthanum cuprate are observed in the underdoped regime⁵, however, both low-energy incommensurate neutron scattering peaks and high-energy commensurate $[\pi, \pi]$ reso-

nance for the bilayer yttrium cuprate in the normal state are detected⁶. These experimental results highlight the importance of some sort of coupling between the CuO_2 planes within a unit cell. It is believed that all these experiments produce interesting data that introduce the important constraints on the microscopic models and theories.

The charge transport of doped single layer cuprates has been addressed from several theoretical viewpoints^{7,8}. Based on the charge-spin separation, an attractive proposal is spinons and holons as basic low-energy excitations, serving as the starting point for the gauge-theory approach⁷. It has been shown⁷ within the t - J model that above the Bose-Einstein temperature, the boson inverse lifetime due to scattering by the gauge field is of order T , which suppresses the condensation temperature and leads to a linear T resistivity. On the other hand, the spin-fermion model near the antiferromagnetic instability has been developed to study the normal-state properties of doped cuprates⁸. This spin-fermion model describes low-energy fermions interacting with their own collective spin fluctuations. Within this approach⁸, the anomalous transport of doped single layer cuprates has been studied extensively⁸, and the results are consistent with the experiments.

As regards an intracell hopping, the band splitting in doped bilayer cuprates was shown by the band calculation⁹, and clearly observed^{10,11} recently by the angle-resolved-photoemission spectroscopy in the doped bilayer cuprate $\text{Bi}_2\text{Sr}_2\text{CaCu}_2\text{O}_{8+\delta}$ above T_c . This bilayer band splitting is due to a nonvanishing intracell coupling. Moreover, the magnitude of the bilayer splitting is constant over a large range of dopings¹¹. Considering these

highly unusual normal state properties in the underdoped regime^{1,2,5,6}, a natural question is what is the effect of the intracell coupling on the normal state properties of doped bilayer cuprates. This is a challenge issue since the mechanism for the superconductivity in doped cuprates has been widely recognized to be closely related with the anisotropic normal-state properties¹². Based on the t - J model, the charge transport and spin response of doped single layer cuprates in the underdoped regime have been discussed¹³⁻¹⁵ within the fermion-spin theory¹⁶, and the obtained results are consistent with experiments¹⁷. In this paper, we apply this successful approach to study the charge transport of the underdoped bilayer cuprates. Our results show that although the bilayer interaction leads to the band splitting in the electronic structure, the qualitative behavior of the conductivity and resistivity is the same as in the single layer case. The conductivity shows the non-Drude behavior at low energies and anomalous midinfrared band separated by the charge-transfer gap, while the temperature dependent resistivity in the heavily underdoped regime is characterized by a crossover from the high temperature metallic-like to the low temperature insulating-like behaviors.

We start from the bilayer t - J model, which can be written as,

$$H = -t \sum_{ai\hat{\eta}\sigma} C_{ai\sigma}^\dagger C_{ai+\hat{\eta}\sigma} - t_\perp \sum_{i\sigma} (C_{1i\sigma}^\dagger C_{2i\sigma} + \text{h.c.}) \\ - \mu \sum_{ai\sigma} C_{ai\sigma}^\dagger C_{ai\sigma} + J \sum_{ai\hat{\eta}} \mathbf{S}_{ai} \cdot \mathbf{S}_{ai+\hat{\eta}} \\ + J_\perp \sum_i \mathbf{S}_{1i} \cdot \mathbf{S}_{2i}, \quad (1)$$

where $\hat{\eta} = \pm\hat{x}, \pm\hat{y}$ within the plane, $a = 1$ and 2 is plane indices, $C_{ai\sigma}^\dagger$ ($C_{ai\sigma}$) is the electron creation (annihilation) operator, $\mathbf{S}_{ai} = C_{ai}^\dagger \vec{\sigma} C_{ai}/2$ are spin operators with $\vec{\sigma} = (\sigma_x, \sigma_y, \sigma_z)$ as Pauli matrices, and μ is the chemical potential. The bilayer t - J model (1) is defined in the subspace with no doubly occupied sites, *i.e.*, $\sum_\sigma C_{ai\sigma}^\dagger C_{ai\sigma} \leq 1$. The strong electron correlation in the t - J model manifests itself by this single occupancy on-site local constraint⁴. To deal with the local constraint in analytical calculations, the fermion-spin theory¹⁶, $C_{ai\uparrow} = h_{ai}^\dagger S_{ai}^-$ and $C_{ai\downarrow} = h_{ai}^\dagger S_{ai}^+$, has been proposed, where the spinless fermion operator h_{ai} keeps track of the charge (holon), while the pseudospin operator S_{ai} keeps track of the spin (spinon), then it naturally incorporates the physics of the charge-spin separation. In this case, the low-energy behavior of the bilayer t - J model (1) in the fermion-spin representation can be rewritten as,

$$H = t \sum_{ai\hat{\eta}} h_{ai+\hat{\eta}}^\dagger h_{ai} (S_{ai}^+ S_{ai+\hat{\eta}}^- + S_{ai}^- S_{ai+\hat{\eta}}^+) \\ + t_\perp \sum_i (h_{1i}^\dagger h_{2i} + h_{2i}^\dagger h_{1i}) (S_{1i}^+ S_{2i}^- + S_{1i}^- S_{2i}^+)$$

$$+ \mu \sum_{ai} h_{ai}^\dagger h_{ai} + J_{\text{eff}} \sum_{ai\hat{\eta}} \mathbf{S}_{ai} \cdot \mathbf{S}_{ai+\hat{\eta}} \\ + J_{\perp\text{eff}} \sum_i \mathbf{S}_{1i} \cdot \mathbf{S}_{2i}, \quad (2)$$

with $J_{\text{eff}} = J[(1-\delta)^2 - \phi^2]$, $J_{\perp\text{eff}} = J_\perp[(1-\delta)^2 - \phi_\perp^2]$, the holon particle-hole order parameters $\phi = \langle h_{ai}^\dagger h_{ai+\hat{\eta}} \rangle$ and $\phi_\perp = \langle h_{1i}^\dagger h_{2i} \rangle$, δ is the hole doping concentration, and S_{ai}^+ (S_{ai}^-) is the pseudospin raising (lowering) operator. Since the single occupancy local constraint has been treated properly within the fermion-spin theory, this leads to disappearing of the extra gauge degree of freedom related with this local constraint under the charge-spin separation¹⁶. In this case, the charge fluctuation couples only to holons^{13,14}. However, the strong correlation between holons and spinons is still included self-consistently through the spinon's order parameters entering the holon's propagator, therefore both holons and spinons are responsible for the charge transport. In this case, the conductivity can be expressed as $\sigma(\omega) = -\text{Im}\Pi^{(h)}(\omega)/\omega$, with $\Pi^{(h)}(\omega)$ is the holon current-current correlation function, and is defined as $\Pi^{(h)}(\tau - \tau') = -\langle T_\tau j^{(h)}(\tau) j^{(h)}(\tau') \rangle$, where τ and τ' are the imaginary times, and T_τ is the τ order operator. Within the Hamiltonian (2), the current density of holons is obtained by the time derivation of the polarization operator using Heisenberg's equation of motion as,

$$j^{(h)} = 2\chi e t \sum_{ai\hat{\eta}} \hat{\eta} h_{ai+\hat{\eta}}^\dagger h_{ai} \\ + 2\chi_\perp e t_\perp \sum_i (R_{2i} - R_{1i})(h_{2i}^\dagger h_{1i} - h_{1i}^\dagger h_{2i}), \quad (3)$$

where R_{1i} (R_{2i}) is lattice site of the CuO_2 plane 1 (plane 2), $\chi = \langle S_{ai}^+ S_{ai+\hat{\eta}}^- \rangle$ and $\chi_\perp = \langle S_{1i}^+ S_{2i}^- \rangle$ are the spinon correlation functions, and e is the electronic charge, which is set as the unit hereafter. The holon current-current correlation function can be calculated in terms of the holon Green's function $g(k, \omega)$ as in the single layer case^{13,14}. However, in the bilayer system, because there are two coupled CuO_2 planes, then the energy spectrum has two branches. In this case, the one-particle holon Green's function can be expressed as a matrix $g(i-j, \tau - \tau') = g_L(i-j, \tau - \tau') + \sigma_x g_T(i-j, \tau - \tau')$, with the longitudinal and transverse parts are defined as $g_L(i-j, \tau - \tau') = -\langle T_\tau h_{ai}(\tau) h_{aj}^\dagger(\tau') \rangle$ and $g_T(i-j, \tau - \tau') = -\langle T_\tau h_{ai}(\tau) h_{a'j}^\dagger(\tau') \rangle$ ($a \neq a'$), respectively. Following discussions of the single layer case^{13,14}, we obtain the conductivity of doped bilayer cuprates as $\sigma(\omega) = \sigma^{(L)}(\omega) + \sigma^{(T)}(\omega)$, with the longitudinal and transverse parts are given by,

$$\sigma^{(L)}(\omega) = \frac{1}{N} \sum_k [(2Z\chi t \gamma_{sk})^2 + (2\chi_\perp t_\perp)^2] \times \\ \int_{-\infty}^{\infty} \frac{d\omega'}{2\pi} A_L^{(h)}(k, \omega' + \omega) A_L^{(h)}(k, \omega') \times$$

$$\frac{n_F(\omega' + \omega) - n_F(\omega')}{\omega}, \quad (4a)$$

$$\sigma^{(T)}(\omega) = \frac{1}{N} \sum_k [(2Z\chi t \gamma_{sk})^2 - (2\chi_\perp t_\perp)^2] \times \int_{-\infty}^{\infty} \frac{d\omega'}{2\pi} A_T^{(h)}(k, \omega' + \omega) A_T^{(h)}(k, \omega') \times \frac{n_F(\omega' + \omega) - n_F(\omega')}{\omega}, \quad (4b)$$

respectively, where Z is the coordination number within the plane, $\gamma_{sk} = (\sin k_x + \sin k_y)/2$, and $n_F(\omega)$ is the fermion distribution function. The longitudinal and transverse holon spectral functions are obtained as $A_L^{(h)}(k, \omega) = -2\text{Im}g_L(k, \omega)$ and $A_T^{(h)}(k, \omega) = -2\text{Im}g_T(k, \omega)$, respectively. The full holon Green's function $g^{-1}(k, \omega) = g^{(0)-1}(k, \omega) - \Sigma^{(h)}(k, \omega)$ with the longitudinal and transverse mean-field (MF) holon Green's functions, $g_L^{(0)}(k, \omega) = 1/2 \sum_\nu 1/(\omega - \xi_k^{(\nu)})$ and $g_T^{(0)}(k, \omega) = 1/2 \sum_\nu (-1)^{\nu+1}/(\omega - \xi_k^{(\nu)})$, where $\nu = 1, 2$, and the longitudinal and transverse second-order holon self-energy from the spinon pair bubble are obtained by the loop expansion to the second-order as,

$$\Sigma_L(k, \omega) = \frac{1}{N^2} \sum_{pq} \sum_{\nu\nu'\nu''} \Xi_{\nu\nu'\nu''}(k, p, q, \omega), \quad (5a)$$

$$\Sigma_T(k, \omega) = \frac{1}{N^2} \sum_{pq} \sum_{\nu\nu'\nu''} (-1)^{\nu+\nu'+\nu''+1} \times \Xi_{\nu\nu'\nu''}(k, p, q, \omega), \quad (5b)$$

respectively, with $\Xi_{\nu\nu'\nu''}(k, p, q, \omega)$ is given by,

$$\Xi_{\nu\nu'\nu''}(k, p, q, \omega) = \frac{B_{q+p}^{(\nu')} B_q^{(\nu)}}{32\omega_{q+p}\omega_q^{(\nu)}} \times \left(Zt[\gamma_{q+p+k} + \gamma_{q-k}] + t_\perp[(-1)^{\nu+\nu''} + (-1)^{\nu'+\nu''}] \right)^2 \times \left(\frac{F_{\nu\nu'\nu''}^{(1)}(k, p, q)}{\omega + \omega_{q+p}^{(\nu')} - \omega_q^{(\nu)} - \xi_{p+k}^{(\nu'')}} + \frac{F_{\nu\nu'\nu''}^{(2)}(k, p, q)}{\omega - \omega_{q+p}^{(\nu')} + \omega_q^{(\nu)} - \xi_{p+k}^{(\nu'')}} \right. \\ \left. + \frac{F_{\nu\nu'\nu''}^{(3)}(k, p, q)}{\omega + \omega_{q+p}^{(\nu')} + \omega_q^{(\nu)} - \xi_{p+k}^{(\nu'')}} + \frac{F_{\nu\nu'\nu''}^{(4)}(k, p, q)}{\omega - \omega_{q+p}^{(\nu')} - \omega_q^{(\nu)} - \xi_{p+k}^{(\nu'')}} \right), \quad (6)$$

with $\gamma_k = (\cos k_x + \cos k_y)/2$, $B_k^{(\nu)} = B_k - J_{\perp\text{eff}}[\chi_\perp + 2\chi_\perp^z(-1)^\nu][\epsilon_\perp + (-1)^\nu]$, $B_k = \lambda[(2\epsilon\chi^z + \chi)\gamma_k - (\epsilon\chi + 2\chi^z)]$, $\lambda = 2ZJ_{\text{eff}}$, $\epsilon = 1 + 2t\phi/J_{\text{eff}}$, $\epsilon_\perp = 1 + 4t_\perp\phi_\perp/J_{\perp\text{eff}}$, and

$$F_{\nu\nu'\nu''}^{(1)}(k, p, q) = n_F(\xi_{p+k}^{(\nu'')})[n_B(\omega_q^{(\nu)}) - n_B(\omega_{q+p}^{(\nu')})] \\ + n_B(\omega_{q+p}^{(\nu')})[1 + n_B(\omega_q^{(\nu)})], \\ F_{\nu\nu'\nu''}^{(2)}(k, p, q) = n_F(\xi_{p+k}^{(\nu'')})[n_B(\omega_{q+p}^{(\nu')}) - n_B(\omega_q^{(\nu)})] \\ + n_B(\omega_q^{(\nu)})[1 + n_B(\omega_{q+p}^{(\nu')})],$$

$$F_{\nu\nu'\nu''}^{(3)}(k, p, q) = n_F(\xi_{p+k}^{(\nu'')})[1 + n_B(\omega_{q+p}^{(\nu')}) + n_B(\omega_q^{(\nu)})] \\ + n_B(\omega_q^{(\nu)})n_B(\omega_{q+p}^{(\nu')}), \\ F_{\nu\nu'\nu''}^{(4)}(k, p, q) = [1 + n_B(\omega_q^{(\nu)})][1 + n_B(\omega_{q+p}^{(\nu')})] \\ - n_F(\xi_{p+k}^{(\nu'')})[1 + n_B(\omega_{q+p}^{(\nu')}) + n_B(\omega_q^{(\nu)})], \quad (7)$$

where $n_B(\omega_k^{(\nu)})$ is the boson distribution function, the MF holon excitation $\xi_k^{(\nu)} = 2Z\chi t \gamma_k + \mu + 2\chi_\perp t_\perp(-1)^{\nu+1}$, the MF spinon excitation $(\omega_k^{(\nu)})^2 = \omega_k^2 + \Delta_k^2(-1)^{\nu+1}$, with $\omega_k^2 = A_1\gamma_k^2 + A_2\gamma_k + A_3$, $\Delta_k^2 = X_1\gamma_k + X_2$, and

$$A_1 = \alpha\epsilon\lambda^2(\chi/2 + \epsilon\chi^z), \\ A_2 = \epsilon\lambda^2[(1-Z)\alpha(\epsilon\chi/2 + \chi^z)/Z \\ - \alpha(C^z + C/2) - (1-\alpha)/(2Z)] \\ - \alpha\lambda J_{\perp\text{eff}}[\epsilon(C_\perp^z + \chi_\perp^z) + \epsilon_\perp(C_\perp + \epsilon\chi_\perp)/2], \\ A_3 = \lambda^2[\alpha(C^z + \epsilon^2 C/2) + (1-\alpha)(1+\epsilon^2)/(4Z) \\ - \alpha\epsilon(\chi/2 + \epsilon\chi^z)/Z] \\ + \alpha\lambda J_{\perp\text{eff}}[\epsilon\epsilon_\perp C_\perp + 2C_\perp^z] + J_{\perp\text{eff}}^2(\epsilon_\perp^2 + 1)/4, \\ X_1 = \alpha\lambda J_{\perp\text{eff}}[(\epsilon_\perp\chi + \epsilon\chi_\perp)/2 + \epsilon\epsilon_\perp(\chi_\perp^z + \chi^z)], \\ X_2 = -\alpha\lambda J_{\perp\text{eff}}[\epsilon\epsilon_\perp\chi/2 + \epsilon_\perp(\chi^z + C_\perp^z) + \epsilon C_\perp/2] \\ - \epsilon_\perp J_{\perp\text{eff}}^2/2, \quad (8)$$

where the spinon correlation functions $\chi^z = \langle S_{ai}^z S_{ai+\hat{\eta}}^z \rangle$, $\chi_\perp^z = \langle S_{1i}^z S_{2i}^z \rangle$, $C = (1/Z^2) \sum_{\hat{\eta}\hat{\eta}'} \langle S_{ai+\hat{\eta}}^+ S_{ai+\hat{\eta}'}^- \rangle$, and $C^z = (1/Z^2) \sum_{\hat{\eta}\hat{\eta}'} \langle S_{ai+\hat{\eta}}^z S_{ai+\hat{\eta}'}^z \rangle$, $C_\perp = (1/Z) \sum_{\hat{\eta}} \langle S_{2i}^+ S_{1i+\hat{\eta}}^- \rangle$, and $C_\perp^z = (1/Z) \sum_{\hat{\eta}} \langle S_{1i}^z S_{2i+\hat{\eta}}^z \rangle$. In order to satisfy the sum rule for the correlation function $\langle S_{ai}^+ S_{ai}^- \rangle = 1/2$ in the absence of the antiferromagnetic long range order, a decoupling parameter α has been introduced in the MF calculation, which can be regarded as the vertex correction¹⁸. All these order parameters, decoupling parameter α , and the chemical potential μ have been determined self-consistently, as done in the single layer case¹⁸.

The frequency- and temperature-dependent conductivity is a powerful probe for systems of interacting electrons, and provides very detailed informations of the excitations, which interacts with carriers in the normal-state and might play an important role in the superconductivity. In Fig. 1, we present the results of the conductivity $\sigma(\omega)$ at doping $\delta = 0.05$ (solid line), $\delta = 0.06$ (dashed line), and $\delta = 0.07$ (dotted line) for parameters $t/J = 2.5$, $t_\perp/t = 0.25$, $J_\perp/J = 0.25$ with temperature $T = 0$ in comparison with the experimental data¹⁹ taken on the underdoped YBa₂Cu₃O_{7-x} (YBCO) (inset). The conductivity of bilayer cuprates in the underdoped regime shows a sharp low-energy peak at $\omega < 0.5t$ and the unusual midinfrared band appearing inside the charge-transfer gap of the undoped system. After an analysis, we found that this low-energy peak decays fastly as $\sigma(\omega) \sim 1/\omega$ (non-Drude fall-off) with increasing energies. Moreover, the weight of the midinfrared peak is doping dependent, and the peak position is shifted to low energy

with increasing dopings. For a better understanding of the optical properties of doped bilayer cuprates, we have studied conductivity at different temperatures, and the results at doping $\delta = 0.06$ for $t/J = 2.5$, $t_{\perp}/t = 0.25$, and $J_{\perp}/J = 0.25$ in $T = 0$ (solid line), $T = 0.3J$ (dashed line), and $T = 0.5J$ (dotted line) are plotted in Fig. 2 in comparison with the experimental data¹⁹ taken on the underdoped YBCO (inset). It is shown that $\sigma(\omega)$ is temperature dependent, and the charge-transfer gap is severely suppressed with increasing temperatures, and vanishes at higher temperature ($T > 0.4J$). Our results are in qualitative agreement with the experiments¹⁹. In comparison with the results from Refs.^{13,14}, it is shown that the present conductivity also is qualitatively consistent with these in the single layer case. In the above calculations, we also find that the conductivity $\sigma(\omega)$ is essentially determined by its longitudinal part $\sigma^{(L)}(\omega)$, this is why in the present doped bilayer cuprates the conductivity spectrum appears to reflect the single layer nature of the electronic state^{1,2,13,14}. This is also why the in-plane charge dynamics is rather universal within whole doped cuprates^{1,2}.

Now we turn to discuss the resistivity, which is closely related to the conductivity, and can be obtained as $\rho(T) = 1/\lim_{\omega \rightarrow 0} \sigma(\omega)$. This resistivity has been calculated, and the results at doping $\delta = 0.05$ (solid line), $\delta = 0.06$ (dashed line), and $\delta = 0.07$ (dotted line) for $t/J = 2.5$, $t_{\perp}/t = 0.25$, and $J_{\perp}/J = 0.25$ are plotted in Fig. 3 in comparison with the experimental results²⁰ taken on the underdoped YBCO (inset). These results show that in the heavily underdoped regime, although the temperature-dependent resistivity is characterized by a crossover from the high temperature metallic-like to the low temperature insulating-like behaviors, the nearly temperature linear dependence in the resistivity dominates over a wide temperature range, in agreement with the experimental results²⁰. In comparison with the re-

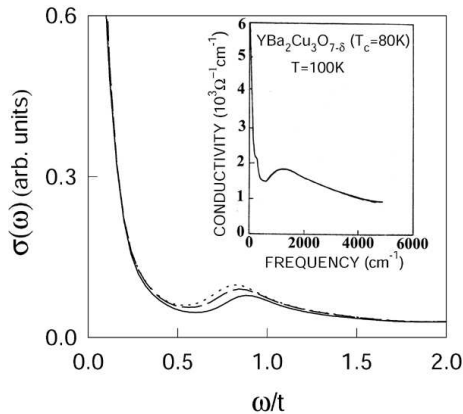


FIG. 1. The conductivity at $\delta = 0.05$ (solid line), $\delta = 0.06$ (dashed line), and $\delta = 0.07$ (dotted line) for $t/J = 2.5$, $t_{\perp}/t = 0.25$, and $J_{\perp}/J = 0.25$ in the zero temperature. Inset: the experimental result on the underdoped $\text{YBa}_2\text{Cu}_3\text{O}_{7-x}$ taken from Ref.¹⁹.

sults from Refs.^{13,14}, it is shown that the present resistivity also is qualitatively consistent with these in the single layer case. We emphasize that since the order parameters, decoupling parameter α , and the chemical potential μ have been determined self-consistently, then these theoretical results were obtained without any adjustable parameters. Furthermore, it is found in the above discussions that the present results are insensitive to the reasonable values of t/J , t_{\perp}/t , and J_{\perp}/J as in the single layer case^{13,14}.

An explanation for the metal-to-insulating crossover in the resistivity in the heavily underdoped regime can be found from the competition between the kinetic energy and magnetic energy in the system. Since cuprate superconducting materials are doped Mott insulators, obtained by chemically adding charge carriers to a strongly correlated antiferromagnetic insulating state, therefore doped cuprates are characterized by the competition between the kinetic energy (t) and magnetic energy (J).

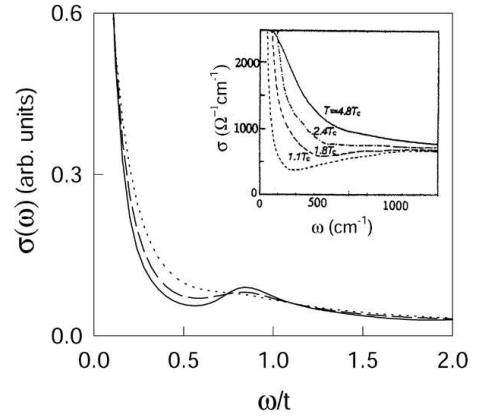


FIG. 2. The conductivity at $\delta = 0.06$ for $t/J = 2.5$, $t_{\perp}/t = 0.25$, and $J_{\perp}/J = 0.25$ in $T = 0$ (solid line), $T = 0.3J$ (dashed line), and $T = 0.5J$ (dotted line). Inset: the experimental result on the underdoped $\text{YBa}_2\text{Cu}_3\text{O}_{7-x}$ taken from Ref.¹⁹.

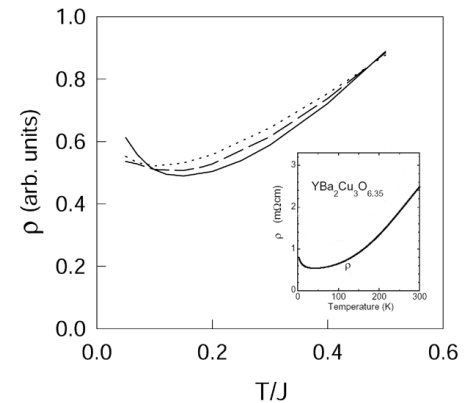


FIG. 3. The resistivity at $\delta = 0.05$ (solid line), $\delta = 0.06$ (dashed line), and $\delta = 0.07$ (dotted line) for $t/J = 2.5$, $t_{\perp}/t = 0.25$, and $J_{\perp}/J = 0.25$. Inset: the experimental result on the underdoped $\text{YBa}_2\text{Cu}_3\text{O}_{7-x}$ taken from Ref.²⁰.

The magnetic energy J favors the magnetic order for spins, while the kinetic energy t favors delocalization of holes and tends to destroy the magnetic order. In the present fermion-spin theory, although both holons and spinons contribute to the charge transport, the scattering of holons dominates the charge transport¹³, where the charged holon scattering rate is obtained from the full holon Green's function (then the holon self-energy (5) and holon spectral function) by considering the holon-spinon interaction, therefore in the heavily underdoped regime the observed crossover from the high temperature metallic-like to the low temperature insulating-like behaviors in the resistivity is closely related with this competition. In lower temperatures, the holon kinetic energy is much smaller than the magnetic energy, in this case the magnetic fluctuation is strong enough to severely reduce the charged holon scattering and thus is responsible for the insulating-like behavior in the resistivity. With increasing temperatures, the holon kinetic energy is increased, while the spinon magnetic energy is decreased. In the region where the holon kinetic energy is much larger than the spinon magnetic energy at higher temperatures, the charged holon scattering would give rise to the temperature linear resistivity.

In summary, we have studied the charge transport in the underdoped bilayer cuprates by considering the bilayer interaction. It is shown that although the bilayer interaction leads to the band splitting in the electronic structure, the qualitative behavior of the charge transport is the same as in the single layer case. The conductivity spectrum shows a low-energy peak and the anomalous midinfrared band. This midinfrared band is suppressed severely with increasing temperatures, while the resistivity exhibits a crossover from the high temperature metallic-like to the low temperature insulating-like behaviors. Our results also show that the mechanism that cause this unusual charge transport in the underdoped cuprates is closely related to the background antiferromagnetic correlations.

ACKNOWLEDGMENTS

This work was supported by the National Natural Science Foundation of China under Grant Nos. 10074007, 10125415, and 90103024, the special funds from the Ministry of Science and Technology of China, and the National Science Council under Grant No. NSC 90-2816-M-032-0001-6.

- ² See, e. g., *Proceedings of Los Alamos Symposium*, edited by K.S. Bedell, D. Coffey, D.E. Meltzer, D. Pines, and J.R. Schrieffer (Addison-Wesley, Redwood city, California, 1990).
- ³ T. Ito, K. Takenaka, and S. Uchida, Phys. Rev. Lett. **70**, 3995 (1993); S. Uchida, Physica C **282-287**, 12 (1997).
- ⁴ P. W. Anderson, in *Frontiers and Borderlines in Many Particle Physics*, edited by R. A. Broglia and J. R. Schrieffer (North-Holland, Amsterdam, 1987), p. 1; Science **235**, 1196 (1987).
- ⁵ K. Yamada, C.H. Lee, K. Kurahashi, J. Wada, S. Wakimoto, S. Ueki, H. Kimura, Y. Endoh, S. Hosoya, and G. Shirane, Phys. Rev. B **57**, 6165 (1998), and references therein.
- ⁶ P. Dai, H.A. Mook, R.D. Hunt, and F. Doğan, Phys. Rev. B **63**, 54525 (2001), and references therein.
- ⁷ N. Nagaosa and P.A. Lee, Phys. Rev. Lett. **64**, 2450 (1990); P.A. Lee and N. Nagaosa, Phys. Rev. B **46**, 5621 (1990).
- ⁸ A. Abanov, A.V. Chubukov, and J. Schmalian, cond-mat/0107421; A. Abanov and A.V. Chubukov, Phys. Rev. Lett. **88**, 217001 (2002); A. Abanov, A.V. Chubukov, and J. Schmalian, Phys. Rev. B **63**, 180510 (2001); R. Haslinger, A.V. Chubukov, and A. Abanov, Phys. Rev. B **63**, 20503 (2001).
- ⁹ O.K. Anderson, A.I. Liechtenstein, O. Jepsen, and F. Paulsen, J. Phys. Chem. Solids **56**, 1573 (1995); A.I. Liechtenstein, O. Gunnarsson, O.K. Anderson, and R.M. Martin, Phys. Rev. B **54**, 12505 (1996).
- ¹⁰ D.L. Feng, N.P. Armitage, D.H. Lu, A. Damascelli, J.P. Hu, P. Bogdanov, A. Lanzara, F. Ronning, K.M. Shen, H. Eisaki, C. Kim, Z.X. Shen, J.-i. Shimoyama, and K. Kishio, Phys. Rev. Lett. **86**, 5550 (2001).
- ¹¹ Y.-D. Chuang, A.D. Gromko, A.V. Fedorov, Y. Aiura, K. Oka, Yoichi Ando, and D. Dessau, cond-mat/0107002; Y.-D. Chuang, A.D. Gromko, A.V. Fedorov, Y. Aiura, K. Oka, Yoichi Ando, H. Eisaki, S.I. Uchida, and D. Dessau, Phys. Rev. Lett. **87**, 117002 (2001).
- ¹² See, e. g., P. W. Anderson, *The Theory of Superconductivity in the High- T_c Cuprates* (Princeton, New Jersey, 1997).
- ¹³ Shiping Feng and Zhongbing Huang, Phys. Lett. A **232**, 293 (1997).
- ¹⁴ Feng Yuan and Shiping Feng, Phys. Lett. A **297**, 235 (2002).
- ¹⁵ Feng Yuan, Shiping Feng, Zhao-Bin Su, and Lu Yu, Phys. Rev. B **64**, 224505 (2001); Shiping Feng and Zhongbing Huang, Phys. Rev. B **57**, 10328 (1998).
- ¹⁶ Shiping Feng, Z.B. Su, and L. Yu, Phys. Rev. B **49**, 2368 (1994); Mod. Phys. Lett. B **7**, 1013 (1993).
- ¹⁷ M.A. Kastner, R.J. Birgeneau, G. Shiran, Y. Endoh, Rev. Mod. Phys. **70**, 897 (1998).
- ¹⁸ J. Kondo and K. Yamaji, Prog. Theor. Phys. **47**, 807 (1972); Shiping Feng and Yun Song, Phys. Rev. B **55**, 642 (1997).
- ¹⁹ J. Orenstein, G.A. Thomas, A.J. Millis, S.L. Cooper, D.H. Rapkine, T. Timusk, L.F. Schneemeyer, and J.V. Waszczak, Phys. Rev. B **42**, 6342 (1990).
- ²⁰ Y. Ando, K. Segawa, S. Komiya, and A.N. Lavrov, Phys. Rev. Lett. **88**, 137005 (2002).

¹ See, e. g., *Physical Properties of High Temperature Superconductors*, edited by D.M. Ginsberg (World Scientific, Singapore, 1994).